Cumulative damage study for the 2010 "blind prediction contest" of a reinforced concrete bridge column

O. Lara & C.E. Ventura
The University of British Columbia, Vancouver

V.A. Suarez
Universidad Técnica Particular de Loja, Ecuador

SUMMARY:
In 2010 PEER, and NEES promoted a "blind prediction contest" of a reinforced concrete bridge column subjected to a set of six earthquake ground motions, tested at the shake table facility of the University of California, San Diego. The test results indicate no flexural failure mechanism for the set of records except Damage Accumulation, DA, in the materials. This was confirmed in the prediction made by Lara, Ventura, and Suarez in 2010 using a fiber finite element model. In this paper the results of additional studies of this problem are presented and discussed. Results of such studies show that three bars fracture due to DA reducing the strength and stiffness of the column. The cyclic damage index, a measure of damage proposed by the first author in 2011 varies from 0.68 to 0.96 and to 1.2 respectively for three consecutive simulations, An index equal to 1.0 indicates that the column is forced to reach one flexural failure mechanism in one run of the scaled set.

1. INTRODUCTION

AASHTO (20011) requires for seismic design of reinforced concrete bridge columns to identify which of the following three flexural failure mechanism controls the design: crushing of the confined concrete, fracture of the longitudinal bars due to tension, or column instability due to P-Δ effect. Lara (2011) demonstrated that during severe earthquakes and aftershocks even columns designed under AASHTO (2007) specifications suffer damage accumulation, DA, inducing considerable reductions of strength and stiffness in the column.

The "blind prediction contest" of a reinforced concrete bridge column, promoted by Peer and Nees in 2010, tested a bridge column under a set of six ground motion records which amplitudes and frequency content were filtered by the shake table. A white noise was applied after each record to keep the response of the column to the previous record. The test was conducted at the University of California, San Diego using the large shake table facility. The prediction by Lara, et al. (2010) deserved from Peer and Nees, (2010) a prize of excellence.

The results of the test indicate that the column under the filtered records did not suffer any of the three flexural failure mechanisms but DA due to strains that resulted in spalling of the unconfined concrete and cracking of the confined concrete, and irrecoverable damage in the steel bars. Research results presented here show that there was an additional DA in the bars induced by cycles of plastic strains reducing the fatigue life in six bars as it was captured by the Finite Fiber Element Model, FFEM, Lara (2011). If two additional consecutive applications of the set shake the column, three bars fracture due to total reduction of their fatigue life, i.e. fracture due to low-cyclic fatigue, reducing the strength and the stiffness of the column by 33% and 50% respectively. A fourth run is applied and more deterioration is observed. To measure DA induced by earthquakes in columns, Lara (2011) introduced the cyclic damage index based on energy dissipation that is calculated here.

1.1 Objective

The main objective of this study is to estimate DA on the tested column and the influence of such accumulation in its strength and stiffness when the column is subjected to the set of the filtered ground motions applied to the column during the test and to repetitions of the set.

1.2 Scope

The tested column was designed not to fail by shear so this study is limited to flexural response. Another limitation is that only the horizontal component of each of the six ground motions of the set was used for the test and so will be used in this study.

2. CHARACTERISTICS OF THE COLUMN AND GROUND MOTIONS USED IN THE TEST

2.1 Characteristics of the column

Figure 1 shows the geometry of the column, the longitudinal and transverse reinforcement and the materials characteristics resulting from tests. The figure also shows the anchorage of the column into the foundation and that of the foundation into the shake table.

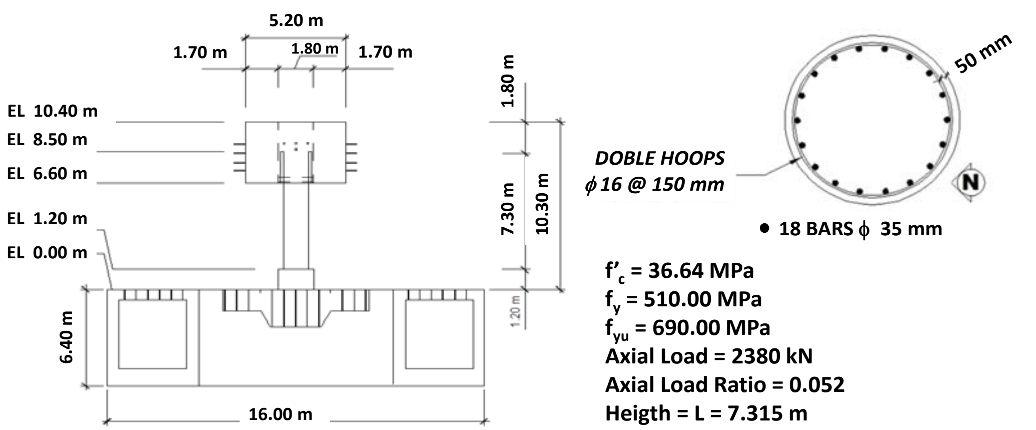

Figure 1 Geometry and material characteristics of the column

2.2 Ground motions

Figure 2 shows the four filtered ground motion records. The sequence of application of the records during the test, according to Peer and Ness (2010) was: Agnews, Corralitos, Los Gatos, Corralitos, Takatori, and Los Gatos. Agnews, Corralitos, and Los Gatos stations recorded the three components of the Loma Prieta 1989 earthquake and Takatori station the components of the Kobe 1995 earthquake.

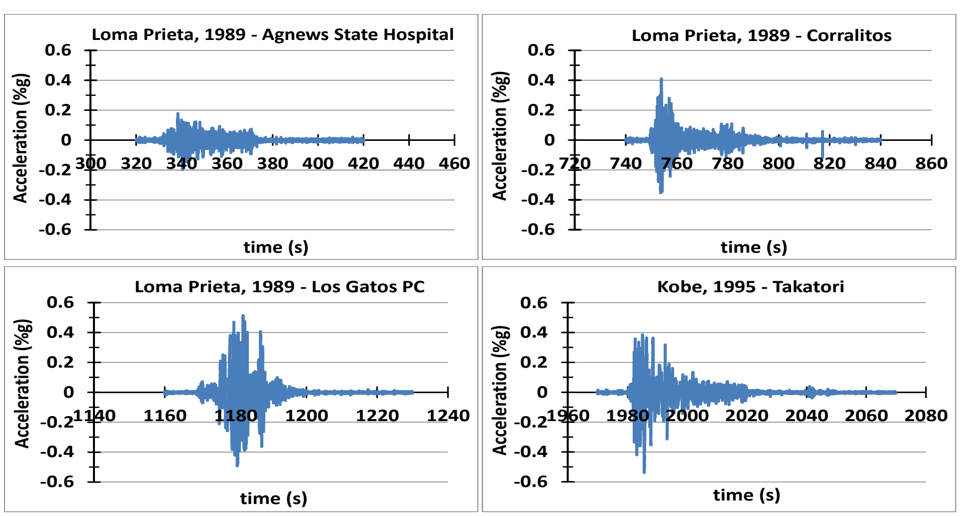

Figure 2. Filtered set of the four ground motions

3. DEFINITION OF FLEXURAL DAMAGE

Lara (2011) has defined flexural damage as the reduction in strength and stiffness in the hysteretic dynamic response of columns. The reduction can occur due to one or more of the following flexural failure mechanisms: the three specified for design by AASHTO (2007), and damage accumulation, DA, that could be, after more studies, an additional mechanism for design as suggested by Lara (2011). DA is due to post-elastic strains in the confined concrete and in the steel bars, and mainly due to the number of cycles of plastic response and reversals that reduce the fatigue life of the bars. If the strains in the confined concrete reach their ultimate value, Mander, et al. (1988), buckling of the bars can occur and this is another mechanism that will reduce strength and stiffness of the column.

4. DAMAGE ACCUMULATION DUE TO CYCLIC RESPONSE IN THE STEEL BARS

Damage accumulation, DA, due to cycles of plastic response is a physical phenomenon not considered by seismic codes around the world. Its effect is to reduce the fatigue life in the bars and it is measured using the plastic strain response, Lara (2011). DA is calculated using equation (1), Manson (1953) and Coffin (1954) where: N_f is the number of cycles with plastic strain amplitude ε_i, and ε_0 is the strain amplitude at which one complete cyclic on a virgin material will cause fracture of the longitudinal steel bar.

$$\varepsilon_i = \varepsilon_0[n_i / N_{fi}]^m \tag{1}$$

$$m = -log\varepsilon_i / logN_{fi} \tag{2}$$

Lara (2011) calibrated the values for ε_0, that it is equal to 0.08 for the 35mm diameter bars, and for m that is equal to -0.37. The calibrated values coincide well with those obtained experimentally by Brown and Kunnath (2004).

Damage, D, in the bars is calculated as the ratio of the number of cycles n_i with plastic strain amplitude ε_i to the number of cycles Nf_i of constant strain ε_i that cause fracture of the bar, equation (3), Miner (1945). The summation of those ratios gives the total damage accumulated at the end of the ground motion.

$$D = \sum \frac{n_i}{N_{fi}} \tag{3}$$

5. THE FIBER FINITE ELEMENT MODEL, FFEM

Figure 3(a) shows the 3-D Finite Fiber Element Model, FFEM, proposed by Lara (2011). The model contains three beam-column elements, Taucer, Scapone and Filippou (1991) that simulates: the strain penetration, L_{sp}, of the longitudinal steel bars into the foundation, the inelastic response of the column along the length of the plastic hinge, L_p, and the elastic upper part of the column. Figure 3(b) shows the section of the column located the ends of each element that is characterized by 328 fiber elements and one additional fiber element for each longitudinal bar. To allow for the rotation of the plastic hinge, a support that restricts translation but allows rotation is located in the interface between element two and the foundation at both sides of the column. Each fiber contains the monotonic characteristics of the materials: stress-strain curves of the confined and unconfined concrete, Mander, et al. (1988), and of the steel bars, Giufree, Menegotto and Pinto (1970, 1973). The FFEM also contains the P-Δ model included in OpenSees (1997) and the damage accumulation model associated to the fatigue counting method proposed by Uriz and Mahin (2008). The FFEM captures the initiation of buckling when the confined concrete reaches the ultimate strain capacity, Mander, et al. (1988).

The OpenSees framework (Open System for Earthquake Engineering Simulation) that is an Object-oriented Finite Element Program (1997), Mazzoni et al. (2006) and McKenna (1997) is used for the simulation of earthquake response of the column.

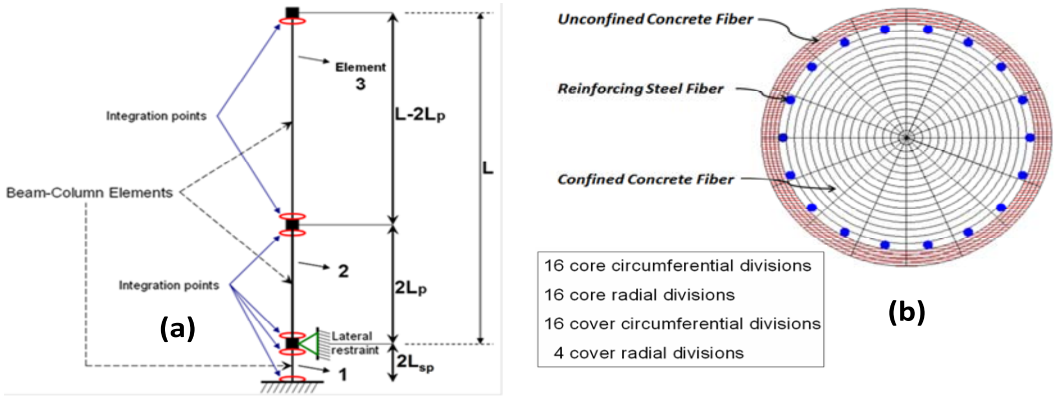

Figure 3. (a) Proposed FFEM using a three element model including strain penetration; (b) Fiber Section

6. CYCLIC DAMAGE INDEX, CDI

The CDI in columns is a measure of damage as above defined and it is calculated using the hysteretic energy dissipated at the end of the ground motion, Lara (2011), through the following equation:

$$CDI = \frac{E_{ucpe}}{E_c} + \beta_c \frac{E_{ucpr}}{E_c} \tag{4}$$

The total energy dissipated at the end of the set of ground motions is separated into E_{ucpe}, the energy dissipated through the new cyclic plastic displacements and E_{ucpr}, the energy dissipated through the repeated cyclic plastic displacements. According to Mahin and Bertero (1972) the damage due to each new cyclic plastic displacement is larger than that induced by each repeated cyclic plastic displacement. E_c is the energy dissipation capacity of the column. The CDI can be estimated for all the structural elements of a system so a global CDI can be obtained.

β_c is a parameter calculated for the column and for the set of ground motions which has been scaled until one of the four flexural failure mechanisms occurs. This occurrence is defined by Lara (2011) as a Significant Damage Performance Level, SDPL, for which the CDI becomes equal to 1.0, and β_c is calculated, equation (4).

Since β_c is associated to SDPL it remains the same for any other scaling of the record but the response will be different changing the CDI to values above or below 1.0. β_c, also measures the importance of the repeated cyclic plastic displacements on the damage accumulation.

7. AASHTO LIMITS FOR DESIGN

According to AASHTO (2007) the requirements for design are: $\varepsilon_c < \varepsilon_{cu}$, $\varepsilon_s < \varepsilon_{su}$, and P-Δ < 0.25$M_p$. Research by Priestley, Calvi, and Kowalski (2007) suggests that P-Δ < 0.33M_p value that will be used in this study. ε_c is the maximum confined concrete strain demand, ε_{cu} is the ultimate compressive confined concrete strain capacity, Mander, et al. (1988), and for the tested column ε_{cu} = 0.02. ε_s is the maximum steel strain demand, ε_{su} is the ultimate tensile strength of the steel bars and its value as specified by AASHTO (2007) varies with the diameter of the bar. For the 35mm bar diameter, ε_{su} = 0.09. P is the maximum axial load demand and M_p is the ultimate flexural moment capacity. According to ASHTO (2007) the above limits must be related to the lateral monotonic force-displacement capacity of the column. There is no specification for DA in AASHTO (2007).

8. ENERGY DISSIPATION CAPACITY

It is the energy dissipated by a virgin column due to a displacement function that induces a failure mechanism at the end of just one complete cyclic displacement response, Lara (2011), Figure 4(a). Table 1 shows that strains in the bars and in the confined concrete and the maximum displacement are less than the limits imposed by AASHTO (2007). Figure 4(b) indicates that there is fracture of bar number 1 due to DA inducing total reduction of its fatigue life at the end of one cycle so this is the only flexural failure mechanism due to the displacement function.

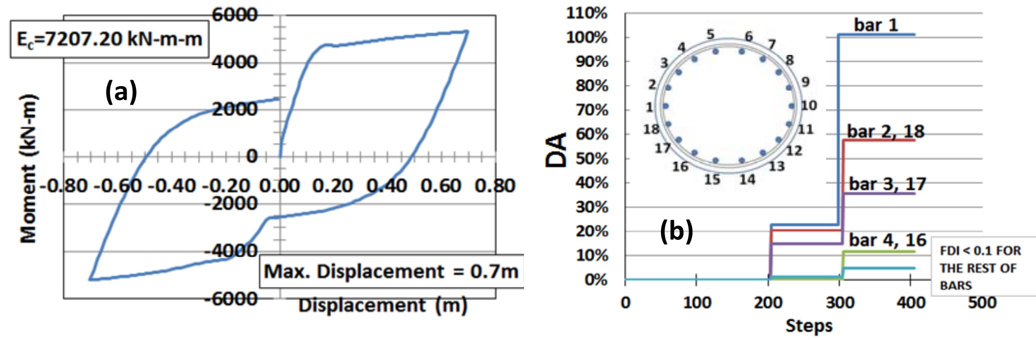

Figure 4. Energy capacity, (a) One complete cycle hysteresis; (b) DA or reduction of fatigue life of the bars in one complete cycle

Table 1. One cycle hysteresis response: maximum values

One Cycle Hysteresis to determine Energy dissipation capacity							
Máx. Displacement, u_m (m)	Máx. Flexural Moment, M (KN-m)	Máx. Shear Force, V (KN)	Máx. Tensile Strain of Bar #1, ε_s (m/m)	Máx. Compressive Strain close to bar #10 (m/m)	Máx. Fatigue Life Loss / Average 5 bars (%)	Number of fractured bars	Energy Capacity, E_c (kN-m-m)
0.7	5300	724	0.05	0.014	100 (bar # 1) / 40	1 (bar # 1)	7207.20

9. MONOTONIC LATERAL SHEAR AND MOMENT CAPACITY

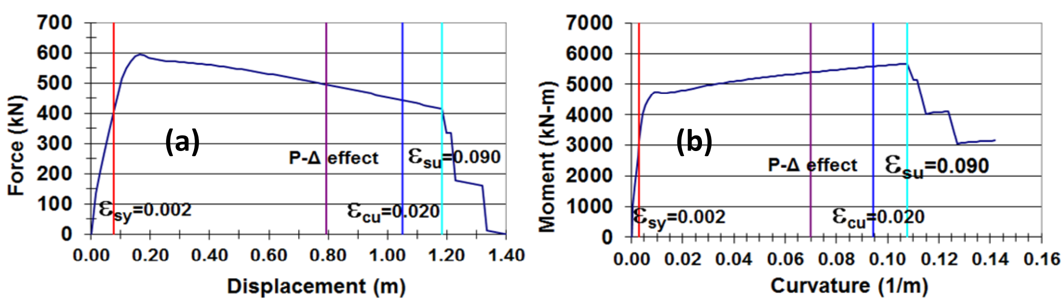

Figure 5. Monotonic capacity of the column, (a) Force-Displacement and; (b) Moment-Curvature

Figure 5(a) shows the force-displacement monotonic capacity of the column with a high of 7.3m and axial load of 2380kN equal to 5% of the axial load ratio. The maximum shear capacity is 600kN and the continuous reduction in shear capacity is due to the P-Δ effect introduced into the FFEM. The limits, AASHTO (2007), for lateral displacement are: 1.05m for ε_{cu} = 0.02, and 1.18m for ε_{su} = 0.09. The ultimate moment capacity, M_p is 5800kN-m, Figure 5(b). Considering P-Δ < $0.33M_p$ the displacement for the column is 80cm so this value controls the design unless during the inelastic dynamic analysis the P-Δ product induces previous instability that is captured by the FFEM.

10. β_c AND SDPL FOR THE COLUMN AND THE SIX FILTERED RECORDS

A scale factor of 1.35 on the set of filtered records is needed to induce SDPL and be able to calculate βc for the column. Table 2 shows that the plastic strains induce DA in the confined and unconfined concrete and in the steel bars but strains and displacements are lower than AASHTO (2007) limits. Figure 6 shows that bar number 1 fracture due to total reduction of its fatigue life and it is the failure mechanism due to the scaled set causing SDPL. The average DA of the next five more fatigued bars is 34%. Knowing the energy capacity, Figure 4(a), and the dissipated energies, Table 2, doing CDI = 1.0, β_c = 0.19, equation (4).

Table 2. Maximum responses to the scaled set. Scale factor, SF = 1.35

Significant Damage Performance Level Analysis						SF for SDPL = 1.35			
	Max. Displacement, u_m (m)	Max. Flexural Moment, M (KN-m)	Max. Shear Force, V (KN)	Máx. Tensile Strain of reinforcement steel bar, ε_s (m/m)	Máx. Compressive Strain of confined concrete, ε_c (m/m)	Máx. Fatigue Life Loss / Average 5 bars (%)	Number of fractured bars	E_{ucpe} (kN-m-m)	E_{ucpr} (kN-m-m)
value	0.620	5356.57	732.27	0.0445	0.0108	100.0 / 45.0	1	4875.40	12600.10
at time	2408.19s (EQ6)	1986.19s (EQ5)	1986.19s (EQ5)	2408.22 (EQ6)	2408.19 (EQ6)	2415.53s (EQ6) - Bar #1	Bar #1		

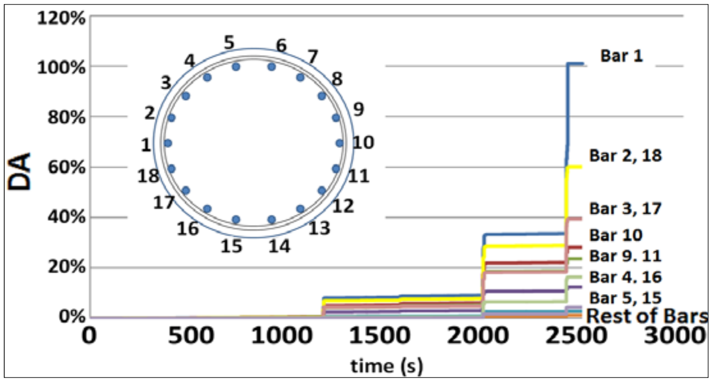

Figure 6. DA of longitudinal bars of the column for the sequence of six filtered records. SF = 1.35, SDPL is fracture of bar 1

11. CICLIC DAMAGE INDEX FOR EACH APLICATION OF THE SET OF RECORDS

11.1 Simulation of the test.

Once SDPL and β_c for the column are known, it is possible now to simulate its response to the set with scale factor = 1.0, as it was applied during the test. Table 3 shows that strains and displacements are less than those of the SDPL and lower than the limits specified by AASHTO (2007). The cyclic plastic strains have induced DA in the materials and some deterioration of stiffness and strength, Figure 7(a). The CDI for the column is 0.68; the DA in bar number 1 is 20% and the DA average of the next five more fatigued bars is 15%, Figure 7(b).

11.2 Damage accumulation in the steel bars and CDI for the second application of the records.

Table 4 shows that the strains in the confined concrete and in the steel have increased inducing deterioration on strength and stiffness of the column, Figure 8(a). The CDI increases from 0.68 to 0.96 due to an increase in DA reaching a very close value to SDPL but, displacements and strains are less than AASHTO (2007) limit values. The increase in DA in the bars is seen in Figure 8(b) that shows that bar number 1 has lost now 61% of its fatigue life while the average loss of fatigue life of the next five more fatigued bars is 40%. There is no failure mechanism.

Table 3. Simulation of Test, SF = 1.0, maximum response values

1st Set of filtered records						SF=1.00	
	Máx. Displacement, u_m (m)	Máx. Flexural Moment, M (KN-m)	Máx. Shear Force, V (KN)	Máx. Tensile Strain of reinforcement steel bar, ε_s (m/m)	Máx. Compressive Strain of confined concrete, ε_c (m/m)	Máx. Fatigue Life Loss / Average 5 bars (%)	Number of fractured bars
value	0.487	5037.8	676	0.0327	0.0081	20.1 / 15.0	0
at time	1986.26s (EQ5)	1986.12s (EQ5)	1986.12 (EQ5)	1986.26 (EQ5)	1986.29 (EQ5)	2417.63s (EQ6) - Bar # 1	-

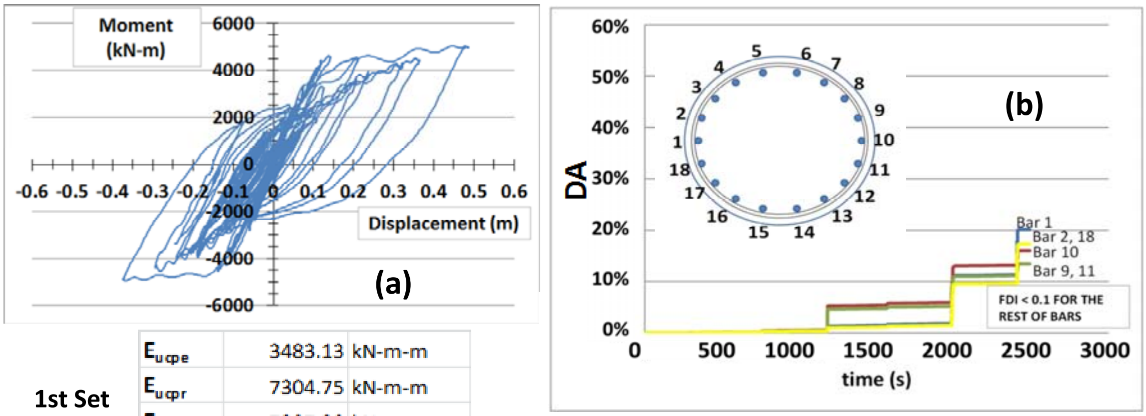

1st Set

E_{ucpe}	3483.13	kN-m-m
E_{ucpr}	7304.75	kN-m-m
$E_{capacity}$	7207.20	kN-m-m
β_c	0.19	
CDI	0.68	

Figure 7. Simulation of the test, SF=1.0; (a) Hysteretic response, and (b) Increment of DA of longitudinal bars of the column for the simulation of the test

Table 4. Response to a second set of records: Maximum values

2nd Set of filtered records				SF=1.00		Results are cummulative	
	Máx. Displacement, u_m (m)	Máx. Flexural Moment, M (KN-m)	Máx. Shear Force, V (KN)	Máx. Tensile Strain of reinforcement steel bar, ε_s (m/m)	Máx. Compressive Strain of confined concrete, ε_c (m/m)	Máx. Fatigue Life Loss / Average 5 bars (%)	Number of fractured bars
value	0.525	5015.94	685.71	0.0363	0.0089	61.5 / 40.0	0
at time	4476.12s (EQ5-2nd set)	4476.08s (EQ5-2nd set)	4476.08s (EQ5-2nd set)	4476.11 (EQ5-2nd set)	4476.07 (EQ5-2nd set.)	4901.12s (EQ6-2nd set) - Bar #1	-

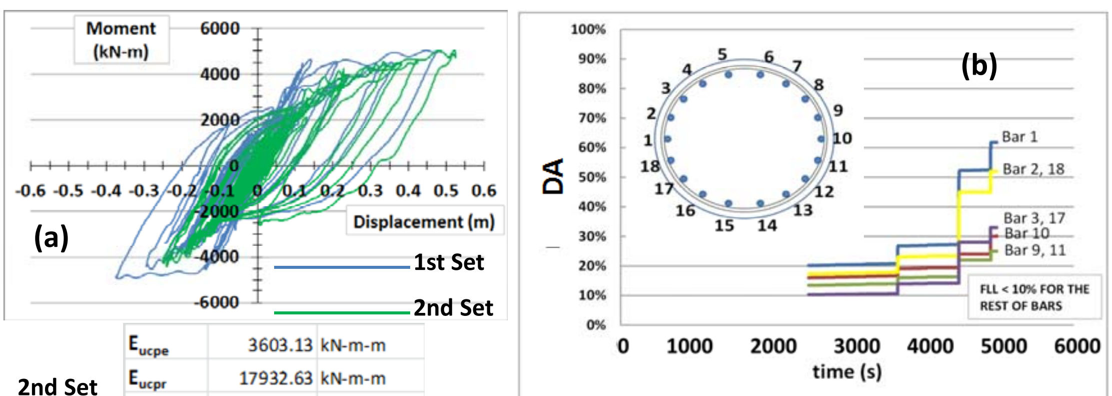

2nd Set

E_{ucpe}	3603.13	kN-m-m
E_{ucpr}	17932.63	kN-m-m
$E_{capacity}$	7207.20	kN-m-m
β_c	0.19	
CDI	0.97	

Figure 8 Two consecutive sets of filtered records, Scale Factor = 1: (a) Hysteretic response; and (b) Increment of DA of longitudinal bars

11.3 Damage accumulation in the steel bars and CDI for the third application of the records.

For this third application, Table 5 shows that strains and displacements are still lower than ASSHTO (2007) limits. Figure 9(a) shows that bars number 1, 2 and, 18 fracture after losing 100% of their fatigue life while the fatigue average of the following five more fatigued bars is 54%. Figure 9(b) shows the reduction in strength and stiffness due to the second and third set. The CDI = 1.2 meaning that the damage, after the third run, is larger than the SDPL.

Table 5. Response to a third set of records: Maximum values

3rd Set of filtered records			SF=1.00			Results are cummulative	
	Máx. Displacement, u_m (m)	Máx. Flexural Moment, M (KN-m)	Máx. Shear Force, V (KN)	Máx. Tensile Strain of reinforcement steel bar, ε_s (m/m)	Máx. Compressive Strain of confined concrete, ε_c (m/m)	Máx. Fatigue Life Loss / Average 5 bars (%)	Number of fractured bars
value	0.525	5107.9	698.27	0.0375	0.0092	100.0 / 54.2	3
at time	6965.96s (EQ5-3rd set)	6965.80s (EQ5-3rd set)	6965.80s (EQ5-3rd set)	6965.95 (EQ5-3rd set)	6965.99 (EQ5-3rd set.)	6965.8s (EQ5-3rd set) - Bar #1, 2, 18	Bar #1, 2 and 18

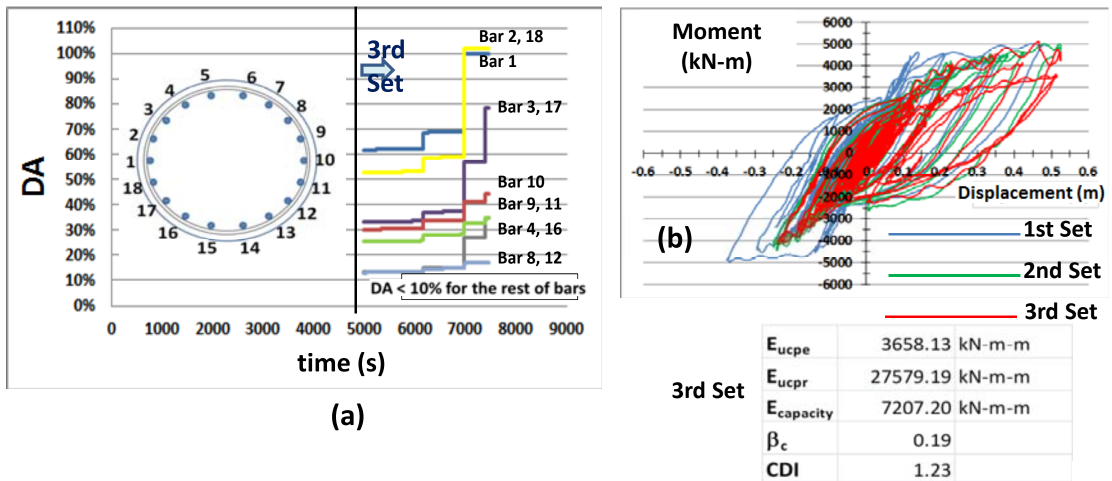

Figure 9 Three consecutive sets of filtered records, Scale Factor = 1: (a) Hysteretic response; and (b) Increment of DA of longitudinal bars

12. COMPARISSON: WITH AND WITHOUT DAMAGE ACCUMULATION MODEL.

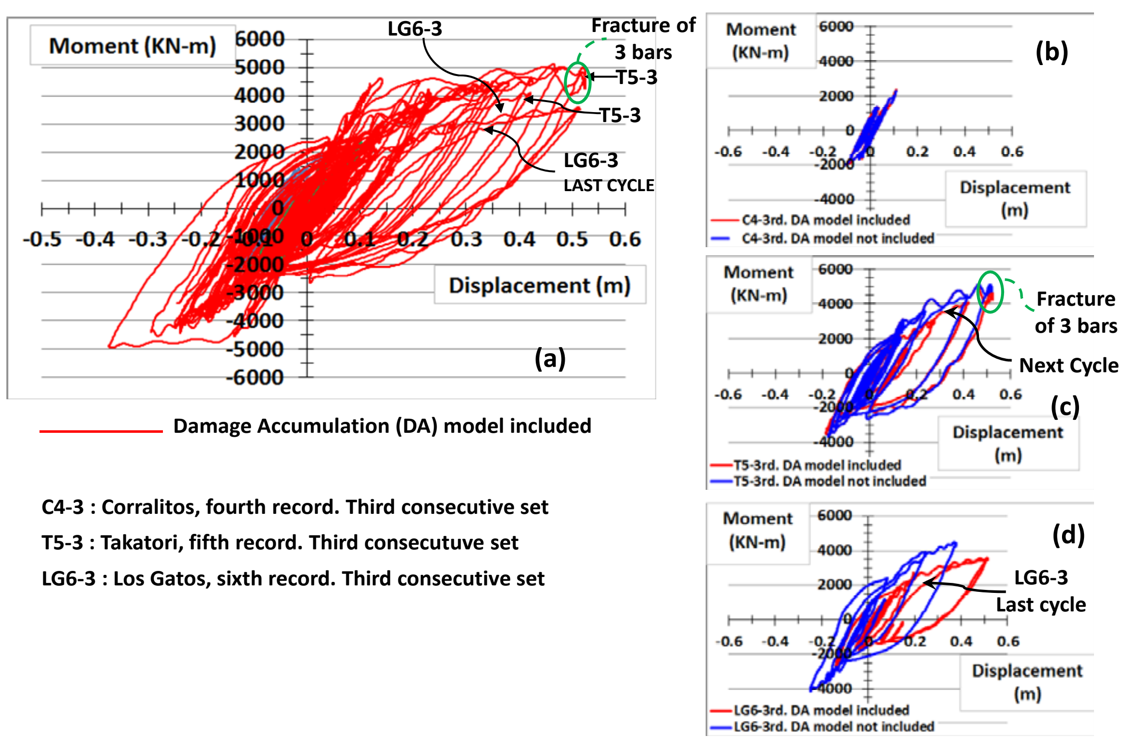

Figure 10 Three consecutive sets of filtered records, Scale Factor = 1.0: (a) hysteretic response; (b), (c) and (d) reduction of strength and stiffness due to DA

Figure 10(a) shows the sequence of damage due to DA during the third consecutive application of the set and Figures 10(b), 10(c), and 10(d) show such sequence in three separate states including a comparison of responses with and without the DA model.

Figure 10(b) shows that up to Corralitos, C3-3, the response is close to elastic and the DA model makes small differences. In Figure 10 (c) the circle shows when three bars fracture due to DA during the Takatori, T5-3, record. The next cycle due to T5-3 shows a reduction of the strength by 20%. Figure 10(d) shows the last cycle during Los Gatos LG6-3 record. The strength reduces by 33% of the maximum demand, Figure 10(a), and the stiffness by 50% of the initial one as seen in Figure 10 (b).

Notice in Figures 10(a) and 10(d) that the strength demand without DA is 4400kN-m, a reduction of 12% of the maximum, but the demand with DA is 3400kN-m, a reduction of 33%. These figures are showing that the reductions due to DA are larger than when DA is not considered.

Figure 11 shows the hysteretic response of the column subjected to four consecutive sets of ground motions. The fourth set causes the fracture of two more bars due to DA during the response to Los Gatos, LG3-4, record and the strength reduces to 44% of the maximum.

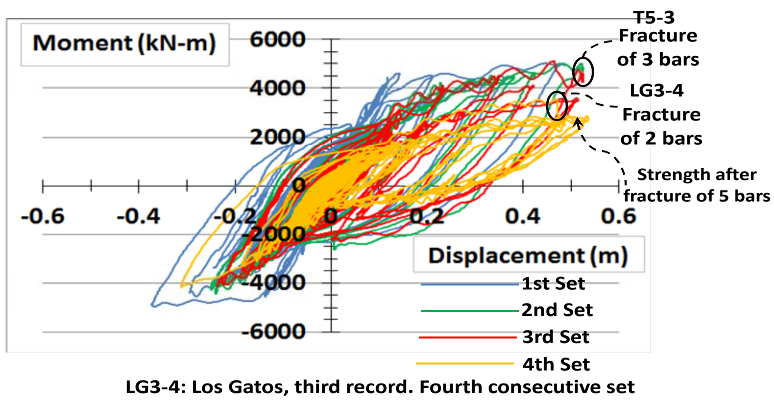

Figure 11 Four consecutive sets of filtered records, Scale Factor = 1 - Hysteretic response

13. CONCLUSIONS

It is demonstrated that bridge columns designed using the 2007 AASHTO (2007) seismic provisions, may not reach any of the three flexural failure mechanisms to be checked for design and mentioned in the introduction of this paper. However, the results presented in this study show that there is damage accumulation, DA, in the column when the post-elastic strains are in the descending branch of the confined concrete curve and in the reversals of the steel bars curves. Both reduce the strength and stiffness of the columns.

The fracture of bars, due to total reduction of their fatigue life is a damage mechanism reducing the strength and stiffness of the column much more than the damage due to post-elastic response in the confined concrete and in the steel. The DA can be considered, after more studies, as an additional flexural failure mechanism to the three specified by AASHTO for design. The Finite Fiber Element Model, FFEM, captures the four mechanisms and also indicates the initiation of buckling when $\varepsilon_c = \varepsilon_{cu}$, Mander, et al. (1988). The maximum confined concrete strain demand for the three runs is in average 0.0087, value lower than $\varepsilon_{cu} = 0.02$. According to previous studies, Lara (2011), and this research, fracture of bars does not increase the maximum displacement response.

The cyclic damage index, based on the use of the energy dissipated by the columns at the end of the ground shaking is a good damage indicator since the hysteretic cycles reflect the damage due to the four mechanisms.

Seismic analysis using models without DA may lead to estimations of strength and stiffness to respond seismic demands considerable higher than those obtained when DA is included in the analysis.

ACKNOWLEDGMENTS

The authors thank Professor Vitelmo V. Bertero who along with Professor Carlos E. Ventura supervised the dissertation of the first author that is the basis of this paper. Professor Bertero provided very valuable comments and suggestions during the preparation of this paper. His permanent advice and support are highly appreciated.

The authors also thank Daniel Toro a research assistant in Sismica Consulting and Member and Secretary of the Ecuadorian Society for Earthquake Engineering. He provided valuable help by running the programs, gathering the data, and preparing the figures.

REFERENCES

American Association of State Highway and Transportation Officials. 2007. Proposed AASHTO Guide Specifications for LRFD Seismic Bridge Design. Subcommittee for Seismic Effects on Bridges T-3. Washington, D.C.

Brown, J., Kunnath, S.K. 2004. "Low-Cycle Fatigue Behavior of Reinforcing Steel Bars". ACI Materials Journal, Vol.101, No.6, 457-466.

Coffin, L. F. Jr. 1954. "A study on the effects of cyclic thermal stresses on a ductile metal". Transactions of the American Society of Mechanicals Engineers. New York, N. Y., 76, pages 931-950.

Giuffre, A. and Pinto, P.E. 1970. "Il Comportamento del Cemento Armato per Sollecitazioni Cicliche di Forte Intensità". Giornale del Genio Civile.

Lara, O. 2011. "The flexural seismic resistant design of reinforced concrete bridge columns". Ph.D. Thesis, University of British Columbia, Vancouver, Canada.

Lara, O., Ventura, C.E., and Suarez, V.A. 2010. Prediction spread sheet submitted for the "Concrete Column Blind Prediction Contest 2010" sponsored by PEER and NEES.

Mahin, S.A. and Bertero, V.V. 1972. "Rate of Loading Effects on Uncracked and Repaired Reinforced Concrete Members". Report No. EERC 72-9. Earthquake Engineering Research Center. College of Engineering. University of California, Berkeley, CA.

Mander, J. B., Priestley, M. J. N., and Park, R. 1988. "Theoretical Stress-Strain Model for Confined Concrete". Journal of Structural Engineering, Vol. 114, Nº 8, ASCE.

Manson, S. S. 1953. "Behavior of materials under conditions of thermal stress". Heat Transfer Symposium, University of Michigan Engineering Research Institute, Ann Arbor, Michigan, pages 9-75.

Mazzoni, S., McKenna, F., Fenves G. L. and et al. 2006. "Open System for Earthquake Engineering Simulation User Manual". *www.opensees.berkeley.edu*.

McKenna Frank. 1997. "Object-Oriented Finite Element Programming: Frameworks for Analysis. Algorithms and Parallel Computing". PhD Thesis, University of California, Berkeley, CA.

Menegotto, M. and Pinto, P.E. 1973. "Method of Analysis for Cyclically Loaded Reinforced Concrete Plane Frames Including Changes in Geometry and Non-Elastic Behavior of Elements under Combined Normal Force and Bending". Proceedings, IABSE Symposium on Resistance and Ultimate Deformability of Structures Acted on by Well Defined Repeated Loads. Lisbon, pp. 15-22.

Miner, M. A. 1945. "Cumulative Damage in fatigue". Journal of Applied Mechanics, Vol. 12, pages A-159.

Pacific Earthquake Engineering Research Center (PEER) and Network for Earthquake Engineering Simulation (NEES). 2010. "Concrete Column Blind Prediction Contest 2010". Column Tested at NEES Large High-Performance Outdoor Shake Table. Englekirk Structural Engineering Center. University of California, San Diego CA. http://nisee2.berkeley.edu/peer/prediction_contest/

Priestley, M. J. N., Calvi, G.M., Kowalsky M. J. 2007. "Displacement-Based Seismic Design of Structures". IUSS Press, Pavia, Italy.

Taucer, F., Spacone, E., and Filippou, F. C. 1991. "A fiber beam-column element for seismic response analysis of reinforced concrete structures". Report No. UBC/EERC-91/17. Earthquake Engineering Research Center. University of California, Berkeley, CA.

Uriz, P., Mahin, S. 2008. "Toward Earthquake-Resistant Design of Concentrically Braced Steel-Frame Structures". Report No. PEER-2008/08. Pacific Earthquake Research Center. University of California, Berkeley, CA.